Electrochimica Acta 483 (2024) 144044

Contents lists available at ScienceDirect

Electrochimica Acta

journal homepage: www.journals.elsevier.com/electrochimica-acta

Model predictive controller of voltage dosage for safe and effective electrochemical treatment of tumors

Mohammad Valibeknejad [a,1], Mahmoud Reza Pishvaie [a], Amir Raoof [b,*]

[a] Department of Chemical and Petroleum Engineering, Sharif University of Technology, Tehran, Iran
[b] Department of Earth Sciences, Utrecht University, Utrecht, the Netherlands

ARTICLE INFO

Keywords:
Electrochemical treatment
Computational transport phenomena
System identification
Generalized predictive control
Liver cancer

ABSTRACT

Electrochemical treatment is an emerging technology that employs direct current to treat cancerous tumors. A significant limitation of this method is the lack of a standardized protocol for voltage application. Our study addresses this by aiming to develop an optimal treatment strategy through the integration of mathematical modeling, numerical simulations, and controller design. We introduce a mathematical model that merges transport equations with electrode kinetics to represent the electrochemical treatment of tumor tissue accurately. The COMSOL software is then utilized to simulate this model, serving as a basis for controller design. Generalized model predictive control is applied to adjust the pH by manipulating the voltage applied to the electrodes. Additionally, we derive a second-order model to predictively characterize the system's behavior. Our designed controller successfully maintains the pH in the electrode's vicinity at a desired level (pH = 2), showcasing robust performance in counteracting disturbances and uncertainties. Analysis of the system's dynamic response reveals an effective ablation zone for the tumor located 5 mm from the anode. By controlling the hydrogen concentration near the anode (up to 5 mm), we ensure the optimal current dosage for efficient tumor ablation, thus minimizing potential harm to adjacent healthy tissues. Our findings offer critical insights into devising an optimal strategy for electrochemical cancer therapy, suggesting significant enhancements in the treatment's efficacy and safety. This proposed method holds promise for broader clinical adoption, potentially revolutionizing electrochemical treatment modalities for cancer.

1. Introduction

Electrochemical therapy (EChT) represents an evolving method for the minimally invasive ablation of tumors and cancers utilizing direct current (DC). This approach offers economic benefits over many conventional treatments, positioning it as a potentially accessible and cost-effective alternative for targeted tumor therapy. The potential of EChT was first demonstrated in 1984 when Bjorn Nordenström successfully applied electrochemical treatment to lung tumors in both benign and malignant cases [1]. EChT specifically targets hyperemic organs through electrolysis, where the application of an electric current at the system's boundary leads to the release of chlorine and oxygen gases, followed by hydrogen production. The dispersion of released protons within the cancerous tissue driven by a concentration gradient (due to diffusion) and an electric field (due to migration) results in a significant pH reduction around the electrode (i.e., the anode), causing the degradation of cancerous tissue. However, this process also poses a risk of collateral damage to healthy tissues due to chlorine production [2–4]. Numerous animal studies [5–12] have explored various aspects of EChT, including electrode spacing, direct current dosage, treatment duration, Coulomb dosage, tumor type, and size. These animal trials have underscored the localized effect and safety of EChT, highlighting the critical role of electrode polarity, inter-electrode distance, electrode distribution, reactions around each electrode, and direct current dose in determining the treatment's effectiveness.

Direct current dose planning is essential for offering this treatment as a predictable and feasible solution. Initially, Nordenstrom's guidelines for dose administration were minimal; therefore, the optimal dose was set at 100 (c/cm of tumor diameter) [13]. Subsequently, Xin modified Nordenstrom's initial dosage according to tumor type (30–100 c/cm) [14]. Reliable dosage can be attained through the use of physiochemical models built on differential equations studying transport phenomena

* Corresponding author.
E-mail address: a.raoof@uu.nl (A. Raoof).
[1] Present address: Utrecht University, Utrecht, the Netherlands,

https://doi.org/10.1016/j.electacta.2024.144044
Received 21 August 2023; Received in revised form 28 February 2024; Accepted 1 March 2024
Available online 1 March 2024

and reactions. These models allow for the simulation of tissue-soluble species concentrations and tissue potential profiles over time, thereby facilitating the prediction of tumor destruction. Given the importance of these models, researchers have proposed various models for optimal dose determination. For example, Gvirn et al. modeled the alkaline environment around a spherical cathode [15], while Berendson and Simonsson studied the distribution of hydrogen ions and molecular chlorine around a spherical anode [16]. These initial models made simplistic assumptions, such as overlooking the potential field's impact on the electrode reaction kinetics and ion distribution. Nilsson proposed the first comprehensive tumor model in 1999, where the tissue was approximated by a sodium chloride (0.16 M) solution under neutral pH conditions. The model considered only the water electrolysis reaction in the electrolyte [17]. Nilsson later modified this model, factoring in the buffer's limiting effect on hydrogen ion release [18]. Further, Nilsson considered the chlorine reactions to investigate the effect of chlorine on the electrochemical treatment of the tumor [19].

Utilizing the mathematical models of the EChT, Pupo et al. developed a three-dimensional model using average healthy and cancerous tissue properties to predict the current generated by varying electrode arrangements [20]. Similarly, Suba et al. developed a two-dimensional model to investigate the impact of electric current from different electrode arrangements on temperature, pH, and the destruction of electrochemically treated tumor tissue [21]. Mokhtare et al. expanded upon these studies, developing a two-dimensional EChT model considering tissue buffering properties and chlorine production reactions. The results revealed that tumor necrosis is a nonlinear function of the applied current's intensity. They further deduced that the oxygen production reaction is the primary source of hydrogen ion production at low direct currents, while water electrolysis dominates hydrogen ion production at high current intensities [22].

1.1. The aim of this study

Despite the exploration of electrochemical cancer treatment through numerous clinical and experimental studies, its widespread acceptance as a standard treatment method has been hindered by several limitations, notably the absence of a reliable protocol for voltage application. This study focuses on overcoming this challenge by ensuring optimal pH coverage over the tumor area while minimizing potential damage to surrounding healthy tissues. A critical aspect of this treatment involves maintaining the concentration of anodically produced hydrogen within a specific range, identified as crucial for achieving therapeutic objectives.

The primary aim of our study is to develop a voltage application scenario, grounded in numerical simulations, that ensures the hydrogen concentration is maintained within a desired range for effective treatment. Given that pH levels are directly correlated with hydrogen concentration, which in turn is influenced by various reactions and transport mechanisms, controlling the rate of hydrogen generation becomes essential. However, factors such as electrode size, type, and surface area, which could influence hydrogen production, are not adjustable during treatment. Consequently, the applied voltage emerges as the sole controllable parameter for adjusting pH levels, which can be strategically increased or decreased to achieve the desired outcome.

To address this, we reformulate Nilsson's model for tumor tissue into a control-oriented framework. This reformulated proxy model is then solved using COMSOL software in cylindrical coordinates, allowing us to analyze the system's open-circuit behavior and its dynamic response to changes in applied voltage. Building on this analysis, we employ the Simulink environment of MATLAB software to design a model predictive controller. This controller is tasked with maintaining the pH level indicative of the hydrogen concentration within a specified range, thereby achieving the desired balance between effective tumor ablation and the preservation of healthy tissue integrity.

2. Methodology

The method utilized in this study is schematically illustrated in Fig. 1 and is briefly explained below. The supplementary material contains more details. This study simulated EChT as a cancer treatment using Nilsson's model [17]. Validation of the proposed model was conducted by Nilsson based on laboratory results. While the mathematical model introduced by Nilsson employs spherical coordinates, our research focuses on simulations and design controllers utilizing cylindrical coordinates. Hence, it was imperative to reframe the governing equations in a control-oriented approach tailored to cylindrical coordinates. The derivation of the control-oriented model (proxy model) is comprehensively elucidated in Section 1 of the supplementary materials.

The proxy model describes EChT by incorporating transport equations and electrode kinetics. The applied voltage in the external circuit was selected as the manipulating variable. The pH at various amplitude points is the system's output, and it can be obtained by inserting pH meters into the tissue (i.e., accessible information in a clinical treatment). The solution domain is considered a cylinder of 25.4 mm in length. To achieve the constant concentration condition at the cathode, the radius of the cylinder is set to 60 mm. Due to symmetry, the simulation is performed in the r direction. The proxy model is simulated using COMSOL software.

A simulated model on the COMSOL platform was used to design a controller. The design of the controller requires information about the dynamic response of the system. The applied voltage (manipulating variable) was varied once as a periodic sinusoidal and once as a periodic step to gain insights into the variation of pH. The system output was defined as the pH values at various locations throughout the tissue. Uncertainties and model disturbances are expected and common in the study of this disease. The body temperature and mass diffusion coefficients of the components are considered disturbances and model uncertainties. The proxy model was simulated at 37 °C. However, during treatment, the patient may experience chills and a fever. Therefore, the sensitivity of the system to these parameters is evaluated.

This study employed the model predictive controller to calculate the proper voltage dosage for the EChT. The model predictive controller is of the GPC (Generalized model predictive control) type. In the optimization section, the Fmincon optimization algorithm is used (additional information and equations regarding the algorithm are provided in the supplementary material Section 3). This method allows users to define the desired linear and nonlinear constraints for the controller. In this study, the constraints are considered as follows (Eqs. (1) and (2)).

$$-0.4 \le \Delta U \le +0.4 \tag{1}$$

$$-1.5 \ge U \ge -3 \tag{2}$$

ΔU represents the growth of the controller output, while U denotes the controller action. Eq. (3) defines the prediction model employed for the GPC controller.

$$y(t) = -a_1 y(t-1) - a_2 y(t-2) + b_1 u(t-1) + b_2 u(t-2) \tag{3}$$

y(t) represents the output of the predictive model at time t, while y(t-1) and u(t-1) respectively denote the output and input of the predictive model at time t-1. The weights of the predictive model (a1, a2, b1, and b2) are calculated through system identification (detailed in Section 2 of the supplementary material). A model predictive controller is designed to regulate the pH at two millimeters from the anode to the set-point value. The cost function for the controller is defined by Eq. (4).

$$J(N_p.N_u) = \sum_{j=1}^{N_p} \delta\left[y(t+j|t) - \hat{W}(t+j)\right]^2 + \sum_{j=1}^{N_u} \lambda[\Delta u(t+j-1)]^2 \tag{4}$$

N_p is the forecast horizon, N_u is the control horizon, δ is the optimization weight for tracking error, λ is the optimization weight for control action, y $(t+j|t)$ is the output of the model at time $t+j$, ΔU is the

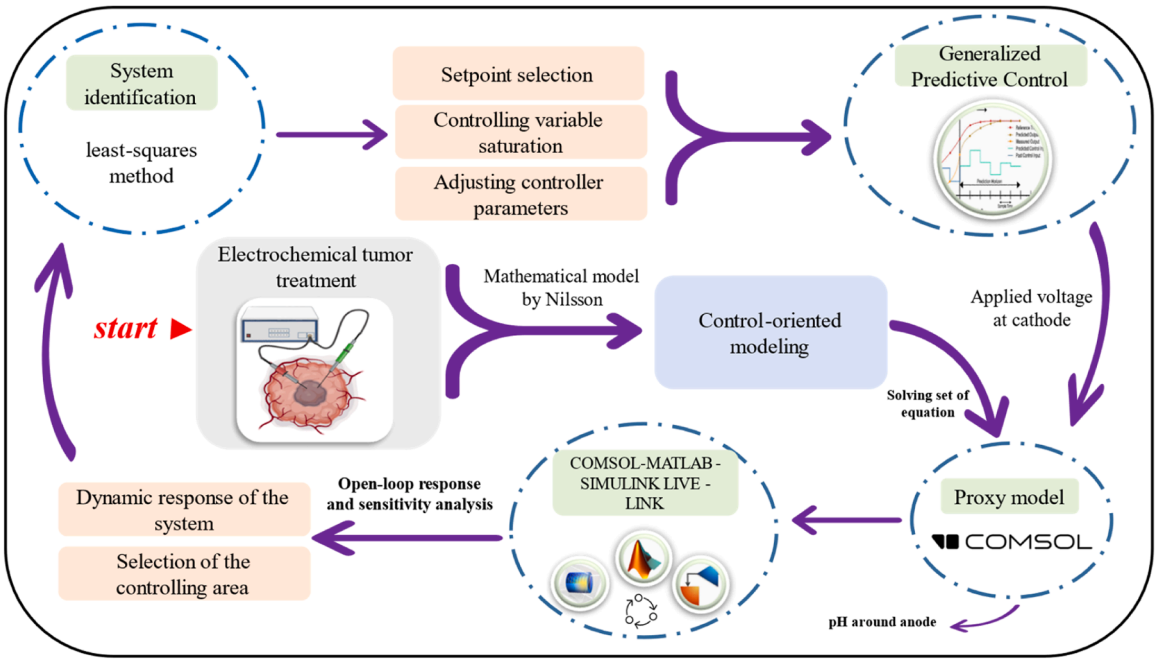

Fig. 1. Sequential steps applied in this study: Initially, Nilsson's models for cancer treatment using electrochemical therapy were reformulated into a control-oriented model in cylindrical coordinates (all simulations and controller designs were performed in cylindrical coordinates). This model was then solved using COMSOL software to elucidate the electrochemical treatment process. Investigation of the system's dynamic response and sensitivity analysis yielded essential inputs for the controller design. After identifying the second-order model as prediction, a Generalized Predictive Controller (GPC) was employed to regulate pH values around the anode, using the applied voltage as the manipulating variable.

growth of the controller output, and $W(t+j)$ is the desired value (set-point). The weights used in the cost function of the GPC controller play a key role in achieving the best performance, which is selected as 1000 for the growth of controller output and 1.8 for the error term. The sampling time was selected as 5 s. The parameters of the model predictive controller are calculated using the equations presented in supplementary material Section 3 and the identified models.

As a predictive model of the system, a second-order model was identified. Identification was performed using the least-squares method described in detail in supplementary material Section 2. A first-order model with delay is required to determine the parameters of the model predictive controller, like forecast horizon and control horizon (equations are presented in supplementary material Section 3). For this purpose, a first-order model of the proxy model has been identified.

Various studies have selected different voltage dosages to evaluate this treatment process. In most of these studies, the scenario of electric current application increases linearly. In this study, according to the existing simulations and related articles, the applied voltage range was selected as: $-3 \leq V \leq -1.5$ [3,23,24]. According to Von Euler, 100 % tissue destruction by acid occurs only at pH <2 [25]. However, studies by Nilsson showed incomplete degradation at pH <3 [18]. As a result, in this study, the prescribed value for eliminating cancerous tissue is considered pH = 2.

This study used COMSOL software to simulate the proxy model and the Simulink environment of the MATLAB software for controller design. The controller (in Simulink) must have access to the proxy model (in COMSOL). Therefore, a live-link connection of MATLAB, Simulink, and COMSOL is required, which is possible for the MATLAB environment. Since the simulations are performed in the Simulink environment of MATLAB software, the Livelink connection between COMSOL and Simulink has been created using the S-function (described in supplementary material Section 4).

3. Results and discussion

3.1. Simulation of proxy model

This section describes the simulation of the proxy model using COMSOL software. The manipulating variable (i.e., the externally applied voltage) is applied according to the defined boundary condition to test the proxy model in an open-loop configuration. The simulation results are presented in Fig. 2. Fig. 2-A shows the distribution of hydrogen ion concentrations at different time intervals. Hydrogen ions are the secondary product of the oxygen synthesis reaction, and they are carried to the electrolyte by migration and diffusion mechanisms. The current density changes over time; high current densities imply an increase in hydrogen production and diffusion to areas with low hydrogen concentrations. An asymmetric distribution of hydrogen concentration is observable due to the disparity in the hydrogen production rate relative to its distribution and spreading. The peak seen in the distribution results from the interaction of the transport process and the electrochemical reaction producing hydrogen. The maximum concentration of hydrogen is observed moving further from the anode over time. Fig. 2-B demonstrates the mass transfer fluxes of hydrogen ions via diffusion and migration processes. As the distance from the anode increases, the gradient in the r-direction in cylindrical coordinates decreases, which results in a decreased rate of hydrogen ion transport. Hydrogen ions with a positive charge move away from the anode. There is a change in the direction of diffusive flux at this point because the electrolyte has the highest concentration of hydrogen ions.

There is a steady rise in chlorine concentration close to the anode, as seen in Fig. 2-C, which depicts the distribution of chlorine concentration. Near the cathode, the concentration reaches its final limit of 0.16 M. Chlorine is transported to the anode by diffusion and migration processes and is consumed at the anode surface due to the production of chlorine molecules. The transfer fluxes of chlorine ions, shown in Fig. 2-D, indicate that both diffusion and migration are directed towards the anode. Fig. 2-E presents the distribution of sodium ion concentrations.

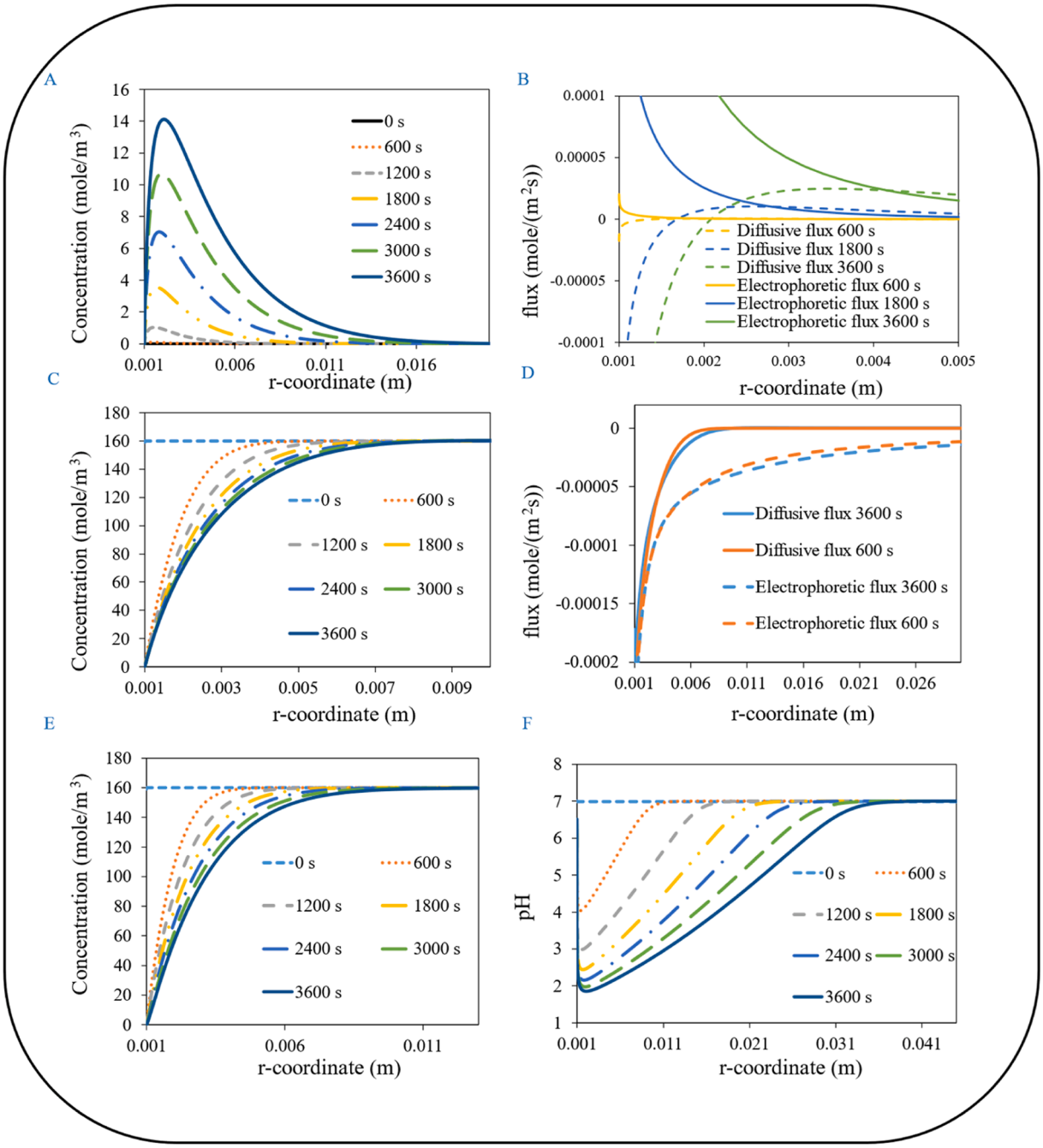

Fig. 2. Concentration and flux profiles of the proxy model: A) Distribution of hydrogen concentration in the domain, B) Mass fluxes of hydrogen ions, C) Distribution of chlorine concentration in the domain, D) Mass fluxes of chlorine ions, E) Distribution of sodium concentration in the domain, and F) pH distribution in the domain.

As mentioned in the modeling section, the mass balance equations for sodium are not solved, and the sodium concentration is computed from the condition of electrolyte neutrality. Owing to the generation of hydrogen ions at the anode and the need for electrical neutrality, the concentration of sodium ions decreases at the anode. Fig. 2-A and Fig. 2-C show that hydrogen concentration decreases with increasing distance from the anode, while chlorine concentration increases, thereby causing an increase in sodium concentration with increased distance from the anode. Fig. 2-F displays the pH distribution in the electrolyte. After 20 min, the pH near the anode drops below three, at which point the destruction of cancerous tissue begins [18,25]. The acidity level is determined by the concentration of hydrogen ions, which is influenced by the induced current. Assuming that a decrease in pH leads to the destruction of cancerous tissue, our proposed controller is designed to administer the optimal voltage, acidifying the environment, and subsequently resulting in cancerous tissue destruction. Our proposed controller manipulates the applied voltage to achieve the desired Coulomb dosage, effectively managing the electric charge delivered to the tissue over time.

3.2. *Open-loop testing*

The system response to step and sinusoidal input is displayed in Fig. 3. The applied voltage (in the form of a step input) in the external circuit and its corresponding outputs are shown in Fig. 3-A and Fig. 3-B, respectively. Hydrogen is produced at the anode and disperses throughout the amplitude via diffusion and migration mechanisms. Due to the gradient decreasing in the r-direction, the voltage's impact on

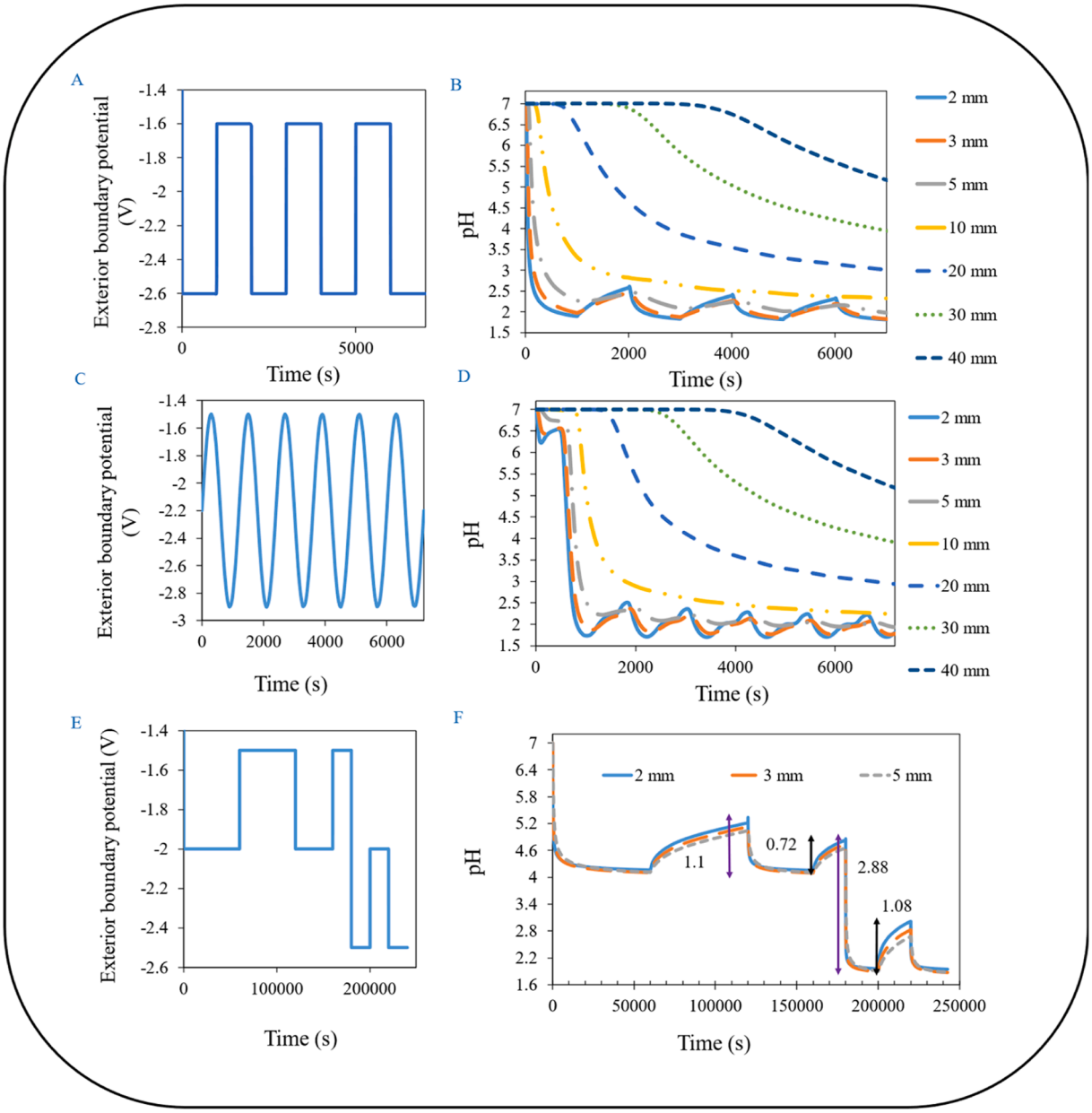

Fig. 3. Open-loop testing of the proxy model: A) Periodic step input applied to the system (voltage applied in the external circuit), B) The response of the pH system to the step input at different points in the tissue, C) Periodic sinusoidal input applied to the system (voltage applied in the external circuit), D) The response of the pH system to the sinusoidal input at different points in the tissue, E) Applied voltage in the external circuit to investigate the system's nonlinear behavior, and F) Nonlinear behavior of the pH system.

hydrogen concentration is anticipated to decrease as the distance from the anode increases. As demonstrated in Fig. 3-B, the response to the input is composed of slow and fast dynamics. When the input (voltage) decreases, hydrogen production also diminishes. To observe a decrease in hydrogen concentration at the output, the hydrogen ions must be transported across the domain by diffusion and migration phenomena, resulting in a slow increase in the pH. When the input (voltage) increases, hydrogen production increases, and the pH responds to the voltage rise rapidly. As presented in Fig. 3-D, the zone affected by the pH in response to the applied voltage (Fig. 3-C) decreases with distance from the anode. Another notable feature is the repetitive and limited cyclical behavior in these areas when exposed to sinusoidal input, which poses challenges to system control. The effect of voltage changes is observed in changes in hydrogen production rate at the anode, which are then transported to other parts of the amplitude with a delay. This delay increases as the distance from the anode grows.

To examine the nonlinearity of the system, the input, as per Fig. 3-E, is applied to the system, and the corresponding output is shown in Fig. 3-F. The system reaches a steady state at −2 Vs for 60,000 s. At this point, a positive half-unit step is applied as the system's input, and the system is allowed to reach a steady state for another 120,000 s. Subsequently, a negative half-unit step is applied to the system's input. Fig. 3-F shows that the system responds to the positive step with slow dynamics, while this response is fast for the negative step. It is evident from Fig. 3-F that the pH response differs for steps of the same magnitude at different operating points.

Sensitivity analysis was conducted for the diffusion coefficient and temperature as uncertainties and disturbances (methodology and results detailed in supplementary material section 5). The results indicated that both factors affect the pH. The proxy model's open-loop response and

sensitivity analysis imply that the proposed controller should address the system's nonlinearities and perform robust against uncertainties and disturbances. The region of effective pH changes diminishes with distance from the anode, which is to be expected considering the cathode is placed at physical infinity. Given our understanding of the pH system behavior in influential areas, it can be decided to select the control area in the regions sensitive to input. This study proposes a distance of 5 mm from the anode, as the input greatly influences these areas and maintains an acidic environment with a pH of less than 3 (suitable for cancer tissue destruction). In EChT, the size of the tumor plays a critical role and is typically assessed before treatment initiation. For larger tumors, multiple electrodes are essential for optimal ablation. Our study defines an effective ablation zone for tumors at 5 mm from the anode. Integrating our findings with existing research [21,26,27] guides electrode orientation for a uniform pH distribution, ensuring effective ablation with minimal impact on healthy cells.

3.3. pH control at a 2 mm distance from the anode

The model delineated in Eq. (3) is utilized as a predictive model, and its corresponding parameters are documented in Table S.2 in the supplementary material. Both the prediction and control horizons were computed using the formula provided in the supplementary material Section 3, yielding values of 10 for the prediction horizon and 3 for the control horizon, based on the models identified in a S.2. Simulations were conducted in the Simulink environment of MATLAB software, with the results depicted in Fig. 4. The set-point tracking for the pH at the 2 mm point is illustrated in Fig. 4-A, showing the effective performance of the designed controller. Fig. 4-B displays the external circuit's applied voltage required to achieve these results.

In earlier sections, the temperature was increased to 40 °C to assess its effect on pH. Mokhtare et al. demonstrate that the tissue temperature can elevate to 44 °C during EChT [22]. In this context, a disturbance is defined as a temperature shift from 37 °C to 35 °C between 25 and 41 min and a change from 35 °C to 44 °C from 41 to 60 min. Fig. 4-C

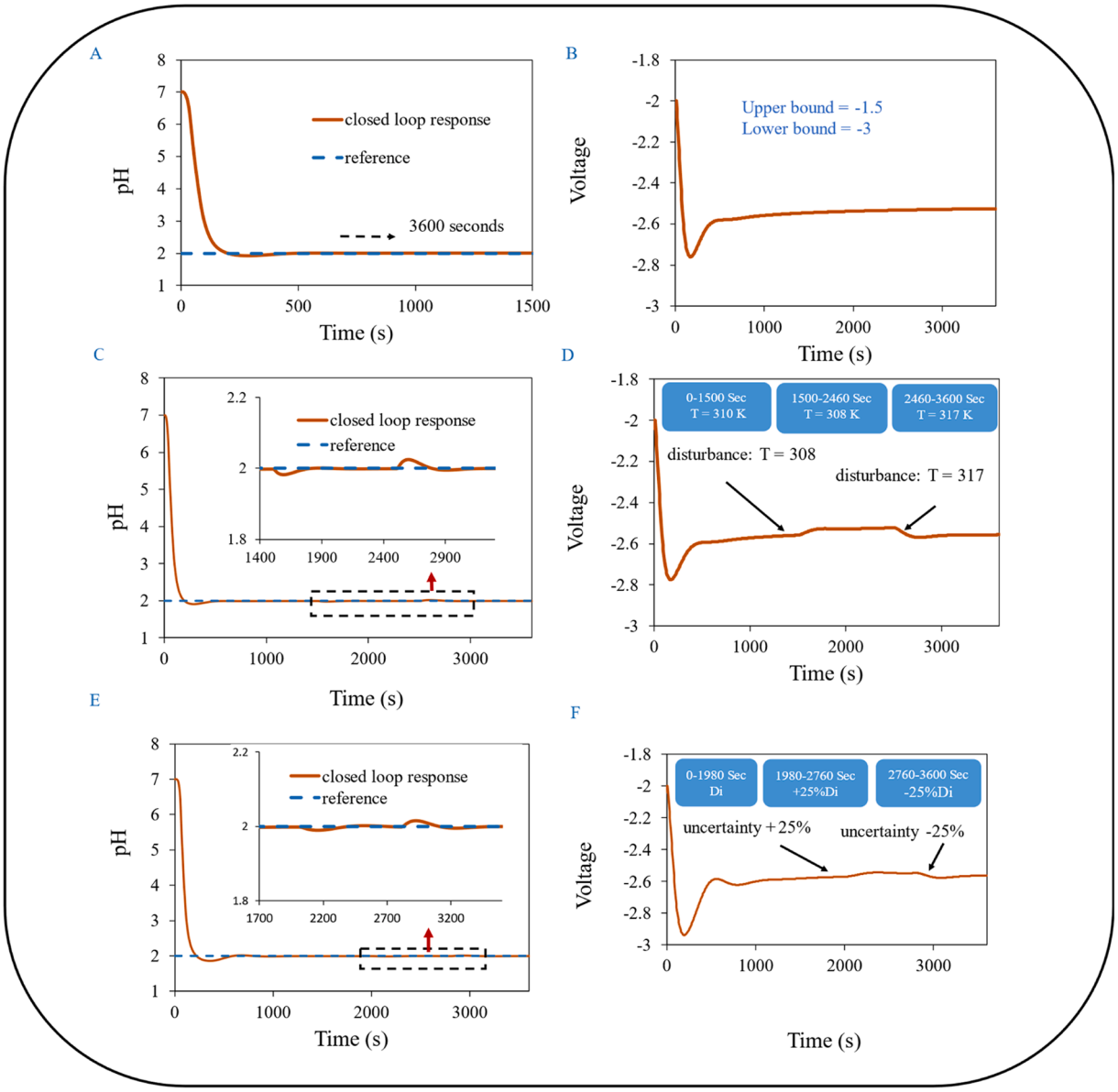

Fig. 4. Controller performance to regulate pH at the 2 mm point: A) Set-point tracking for the 2 mm point, B) Control effort (voltage), C) Tracking of the set-point value in the presence of disturbance by the model predictive controller, D) Applied voltage in the external circuit by the controller, E) Tracking the set-point value in the presence of uncertainty in the model parameters, and F) Applied voltage in the external circuit by the controller.

displays the tracking of the reference pH value considering this disturbance. The magnified section of the diagram clearly shows the controller's capability to counteract the effects of disturbances. The control signal (voltage applied in the external circuit) is demonstrated in Fig. 4-D. To evaluate the controller's efficacy in neutralizing the impact of uncertainty in model parameters, an uncertainty of +/- 25 % is considered for the mass diffusion coefficients at 33 min and 46 min, respectively. Fig. 4-E displays the set-point tracking when considering model parameter uncertainty. The magnified section of the diagram indicates the robust performance of the controller against model uncertainty. The corresponding applied voltage is demonstrated in Fig. 4-F.

3.4. pH control around the anode

The investigation into the dynamic's response to EChT discovered that the tissue surrounding the anode, extending up to 5 mm, exhibits an acidic environment, with the pH response notably sensitive to voltage fluctuations. The aim of this section is to design a GPC controller to manipulate the pH level within a 5 mm span around the anode. To achieve this, control points are selected at distances of 2 mm, 3 mm, and 5 mm from the anode. Eq. (5) shows the cost function for the GPC controller. The tracking error of three points and the controller action are considered in this equation.

$$J(N_p.N_u) = \sum_{j=1}^{N_p} \delta.2[\hat{y}.2(t+j|t) - W.2(t+j)]^2 + \sum_{j=1}^{N_p} \delta.3[\hat{y}.3(t+j|t) - W.3(t+j)]^2 + \sum_{j=1}^{N_p} \delta.5[\hat{y}.5(t+j|t) - W.5(t+j)]^2 + \sum_{j=1}^{N_u} \lambda[\Delta u(t+j-1)]^2 \quad (5)$$

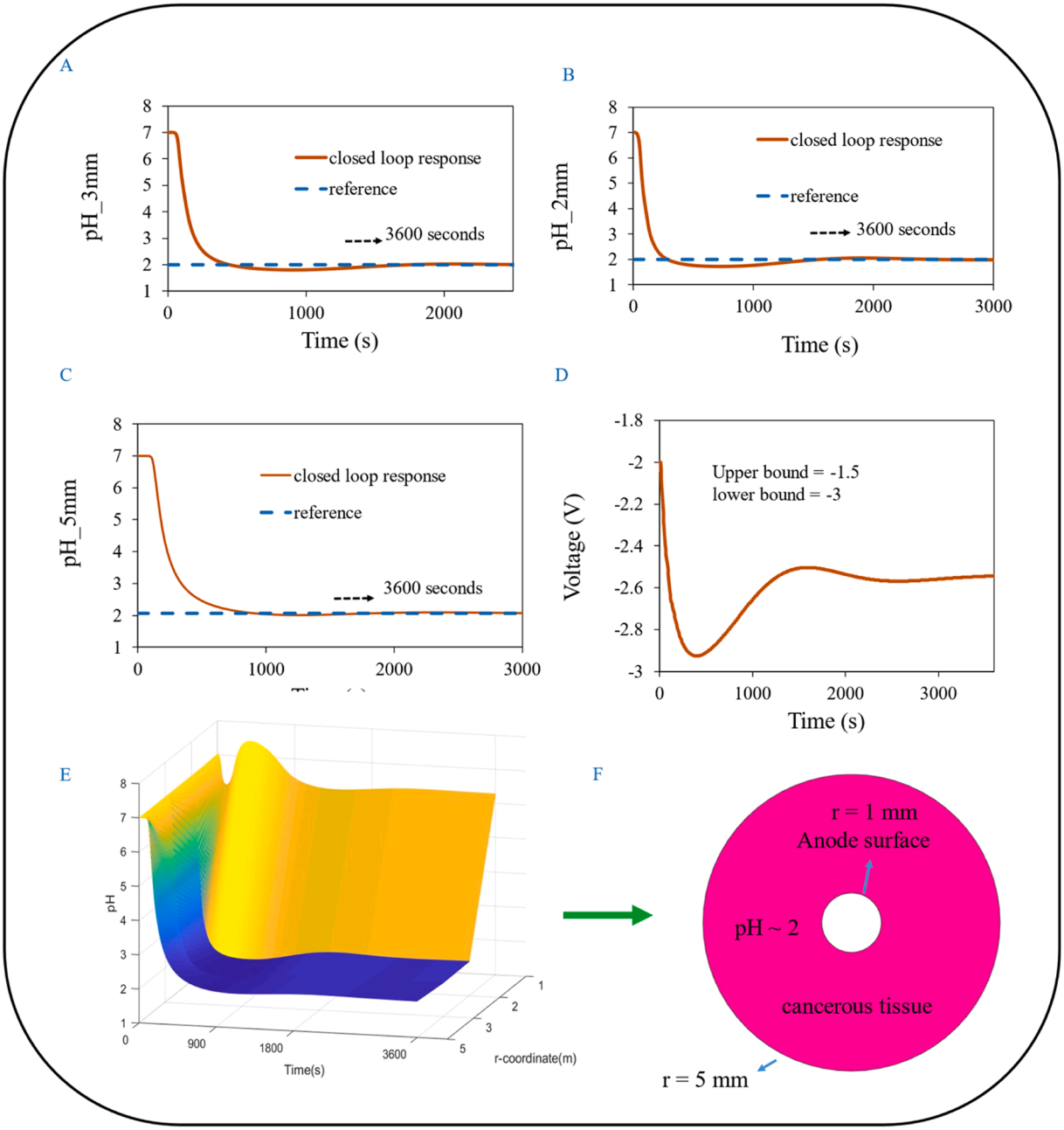

Fig. 5. Regulation of pH values around the anode: tracking the set-point value for A) 2 mm point, B) 3 mm point, and C) 5 mm point. D) Controller-applied voltage in the external circuit, and E) Time-based pH changes around the anode, F) The suitable pH value for tumor degradation around the anode extends up to 5 mm.

In the preceding equation, δ_2, δ_3, δ_5, and λ represent the optimization weights for tracking error at 2, 3, and 5 mm points and the growth of controller output, respectively. N_p is the forecast horizon, N_u is the control horizon, y $(t+j|t)$ is the output of the model at time $t+j$, ΔU is the growth of the controller output, and W$(t+j)$ is the desired value (setpoint). The GPC controller's performance optimization heavily relies on the weightings assigned within its cost function. These weights are selected as follows: 10,000 for control development, 1 for the error at the 2 mm point, 1 for the error at the 3 mm point, and 1.2 for the error at the 5 mm point. Moreover, the forecast horizon is set to 20, the control horizon to 3, and the sampling time to 5 s.

The pH tracking at points 2, 3, and 5 mm, respectively, is shown in Panels A, B, and C of Fig. 5, respectively. These figures show that the controller efficiently tracks the set-point values of 2 at points 2 and 3 mm and 2.06 at point 5 mm. The applied voltage in the external circuit is shown in Fig. 5-D to attain these results. Errors at the 2, 3, and 5 mm points comprise the cost function of the GPC controller. The influence of changes in the controller variable is seen in the output with delay, which is proportional to the distance from the anode. Consequently, the controller initiates additional control commands to adjust the pH at the 5 mm point towards the set-point value. As a result, this leads to a significant undershoot at points nearest to the anode. The GPC controller's weights were set to minimize the required time for the pH at the 5 mm point to reach the set-point value and the undershoot of the 2 and 3 mm points.

Fig. 5-E presents the pH variations in amplitude around the anode. As illustrated, the designed controller successfully maintains the pH close to the set-point value within a 5 mm distance from the anode. Because of the neutral electrolyte condition and decreasing chloride concentration, pH stays constant over time in the vicinity of the anode (1 mm). Three essential substances in EChT, hydrogen chlorite, soluble chlorine, and acids derived from hydrogen ions, such as hydrogen chloride, are responsible for the destruction of cancerous tissue in various areas. Sick tissue is eliminated up to one millimeter away from the anode using hypochlorite and dissolved chlorine. Further electrode distance necessitates an acid-forming environment for tumor ablation. Hydrogen ions and soluble chlorine molecules are essential for the formation of hydrogen chloride. As a result, the controller can manipulate the voltage dosage required for treatment [18,25].

Chlorine and hypochlorite cause destruction within 1 mm, but applied voltage creates an acidic environment that allows tissue destruction up to 5 mm. Increasing the applied voltage gradually helps patients adapt to treatment; this is a common approach used in both human and animal experiments [13,14]. The weights of the cost function were selected in a way to facilitate a stepwise increase in dosage. The controller that has been designed is able to maintain pH values at the desired level by applying voltage within a range that is considered clinically acceptable, which is usually limited to −3 [3,23,24].

It's noteworthy that this study concentrates on the electrochemical treatment of tumor tissue using a single anode and considers only the oxygen and chlorine production reactions at the anode. However, other reactions transpire during this treatment around the electrodes [16–19, 22]. Research indicates that the tumor destruction around the cathode mirrors that around the anode, albeit through a different mechanism [3, 10]. Further research and clinical studies are needed to evaluate the feasibility and effectiveness of the proposed approach. A comprehensive study involving optimal arrangements of the electrodes [20,21], modeling both electrodes and electrolyte reactions [15,17] and interaction between adjacent electrodes is required to arrive at a reliable dosage. This study offers valuable insights into developing an optimal strategy for electrochemical cancer treatment. Integrating mathematical models, numerical simulations, and controller design proposes a promising approach to boost the efficacy and safety of this emerging treatment modality. Further advancements in this field can lead to a wider acceptance of electrochemical therapy as a universal treatment method for various types of cancer.

This study employed a model predictive controller to devise the optimal voltage application scenario, with liver cancer serving as a case study. The methodology established here demonstrates versatility and can be adapted for treating other organs using EChT. In Electroporation (EP)-based protocols, including Electrochemotherapy (ECT), Gene Electrotransfer (GET), and Irreversible Electroporation (IRE), tissue damage during cancer treatment is primarily attributed to temperature and pH variations [28,29]. The model proposed in this study could be instrumental in understanding and controlling pH modulation, ensuring it remains within the optimal range for effective treatment.

4. Conclusions

The clinical potential of electrochemical therapy (EChT) is underscored by its demonstrated efficacy in cancer treatment, as evidenced by animal studies and clinical applications. These investigations have affirmed the method's effectiveness and the importance of precisely applied electric current scenarios. However, due to the complexities inherent in numerical studies, the electrochemical treatment of tumors has largely been confined to experimental settings. A scarcity of fundamental research has impeded broader exploration in this field. Our study sheds light on the path toward a deeper understanding and control of the variables integral to this promising treatment modality. We have identified suitable operating conditions for EChT, informed by previous studies on both animals and humans. Utilizing these parameters, we have designed a controller and modeled it to provide optimal conditions for disease treatment. This controller serves not only as a functional instrument but also as a means to enhance our comprehension of the precise controls required for successful treatment outcomes.

In our research, we adapted Nilsson's mathematical model to cylindrical coordinates with a control-oriented focus. The resulting control-oriented model was simulated using COMSOL software and subsequently used as a basis for controller design in MATLAB software. We employed a model predictive controller to regulate the current dose delivered to the electrodes. The initial step involved identifying a proxy model through the least squares method. A controller was then specifically designed for a 2 mm point using generalized predictive control and the identified models. This controller adeptly maintained the pH at this point at the targeted value of 2, showcasing its robustness and adaptability. To further validate our approach, we extended the controller to include points at 2, 3, and 5 mm. This extension not only confirmed the controller's adaptability but also its capability to maintain the desired pH within a broader range (up to 5 mm), demonstrating its flexibility and potential for application in various treatment scenarios and clinical environments.

The approach proposed in this study carries profound implications for the advancement of electrochemical cancer therapy. It offers critical insights into the development of an optimal treatment strategy, particularly addressing the critical gap of a standardized voltage application protocol. The integration of mathematical modeling with numerical simulations enables the prediction of tumor destruction and the optimization of treatment parameters. Collectively, our study illuminates the promise of EChT, making significant progress in enhancing its efficacy through a controller designed to maintain pH values around the anode up to 5 mm at the desired level, thus facilitating safe tumor ablation. Consequently, this research paves the way for increased acceptance and implementation of electrochemical therapy in the ongoing global battle against cancer.

CRediT authorship contribution statement

Mohammad Valibeknejad: Writing – original draft, Visualization, Software, Methodology, Data curation, Conceptualization. **Mahmoud Reza Pishvaie:** Writing – review & editing, Supervision, Software, Conceptualization. **Amir Raoof:** Writing – review & editing, Software, Methodology, Conceptualization.

Declaration of competing interest

The authors declare that they have no known competing financial interests or personal relationships that could have appeared to influence the work reported in this paper.

Data availability

Data will be made available on request.

Acknowledgment

We extend our gratitude to the Centre for Unusual Collaborations (CUCo) and Structures of Strength (SoS), the platform for unusual collaborations on porous materials, for their invaluable support throughout this study. Their insightful input and suggestions significantly enriched the scope and depth of our work.

Supplementary materials

Supplementary material associated with this article can be found, in the online version, at doi:10.1016/j.electacta.2024.144044.

References

[1] B. Nordenström, Preliminary clinical trials of electrophoretic ionization in the treatment of malignant tumors, IRCS Med. Sci. 6 (1978) 37–40.
[2] G. Garcea, T.D. Lloyd, C. Aylott, G. Maddern, D.P. Berry, The emergent role of focal liver ablation techniques in the treatment of primary and secondary liver tumours, Eur. J. Cancer 39 (2003) 2150–2164, https://doi.org/10.1016/S0959-8049(03)00553-7.
[3] L. Jing-Hong, X.Yu Ling, Electrochemical therapy of tumors, Conf. Pap. Med. 2013 (2013) 1–13, https://doi.org/10.1155/2013/858319.
[4] C. O'Brien, A. Ignaszak, Advances in the electrochemical treatment of cancers and tumors: exploring the current trends, advancements, and mechanisms of electrolytic tumor ablation, ChemElectroChem. 7 (2020) 3895–3904, https://doi.org/10.1002/CELC.202000887.
[5] M. Telló, G.A.D. Dias, A. Cardona, A. Raizer, Tumor compression due application of DC current, IEEE Trans. Magn. 37 (2001) 3753–3756, https://doi.org/10.1109/20.952706.
[6] M. Telló, L. Oliveira, O. Parise, A.C. Buzaid, R.T. Oliveira, R. Zanella, A. Cardona, Electrochemical therapy to treat cancer (in vivo treatment), Annual International Conference of the IEEE Engineering in Medicine and Biology - Proceedings (2007) 3524–3527. https://doi.org/10.1109/IEMBS.2007.4353091.
[7] S.A. Wemyss-Holden, A.R. Dennison, G.J. Finch, P.M. De La Hall, G.J. Maddern, Electrolytic ablation as an adjunct to liver resection: experimental studies of predictability and safety, Br. J. Surg. 89 (2002) 579–585, https://doi.org/10.1046/J.1365-2168.2002.02064.X.
[8] N. Olaiz, F. Maglietti, C. Suárez, F.V. Molina, D. Miklavcic, L. Mir, G. Marshall, Electrochemical treatment of tumors using a one-probe two-electrode device, Electrochim. Acta 55 (2010) 6010–6014, https://doi.org/10.1016/J.ELECTACTA.2010.05.057.
[9] P. Turjanski, N. Olaiz, P. Abou-Adal, C. Suárez, M. Risk, G. Marshall, pH front tracking in the electrochemical treatment (EChT) of tumors: experiments and simulations, Electrochim. Acta 54 (2009) 6199–6206, https://doi.org/10.1016/J.ELECTACTA.2009.05.062.
[10] H.M.C. Ciria, M.M. González, L.O. Zamora, L.E.B. Cabrales, G.V.S. González, L. O. De Oliveira, R. Zanella, A.C. Buzaid, O. Parise, L.M. Brito, C.A.A. Teixeira, M.D. N. Gomes, G. Moreno, V.F. Da Veiga, M. Telló, C. Holandino, Antitumor effects of electrochemical treatment, Chin. J. Cancer Res. 25 (2013) 223, https://doi.org/10.3978/J.ISSN.1000-9604.2013.03.03.
[11] E.A. Schroeppel, K. Kroll, M.C. Damon, A.A.H. Kroll, Direct current ablation destroys multi-stage fibrosarcomas in rats, in: Proceedings of the 31st Annual International Conference of the IEEE Engineering in Medicine and Biology Society: Engineering the Future of Biomedicine 2009, EMBC, 2009, pp. 3099–3104, https://doi.org/10.1109/IEMBS.2009.5332541.
[12] E. Luján, H. Schinca, N. Olaiz, S. Urquiza, F.V. Molina, P. Turjanski, G. Marshall, Optimal dose-response relationship in electrolytic ablation of tumors with a one-probe-two-electrode device, Electrochim. Acta 186 (2015) 494–503, https://doi.org/10.1016/J.ELECTACTA.2015.10.147.
[13] B.E.W. Nordenström, An additional circulatory system: vascular-Interstitial closed electric circuits (VICC), J. Biol. Phys. 15 (1987) 43–55, https://doi.org/10.1007/BF01858151/METRICS.
[14] K.-H. Li, Y.-L. Xin, Y.-N. Gu, B.-L. Xu, D.-J. Fan, B.-F. Ni, Effects of direct current on dog liver: possible mechanisms for tumor electrochemical treatment, Bioelectromagnetics 18 (1997) 2–7, https://doi.org/10.1002/(SICI)1521-186X(1997)18:1.
[15] J. R, D.M.P. Cvirn, Tumour pH changes due to electrotherapy - experimental results and mathematical model, Electrotechn. J. 61 (1994) 37–42.
[16] J. Berendson, D. Simonsson, Electrochemical aspects of treatment of tissue with direct current, Eur. J. Surg. Suppl. (1994) 111–115. https://europepmc.org/article/med/7531012 (accessed August 17, 2023).
[17] E. Nilsson, J. Berendson, E. Fontes, Electrochemical treatment of tumours: a simplified mathematical model, J. Electroanalyt. Chem. 460 (1999) 88–99, https://doi.org/10.1016/S0022-0728(98)00352-0.
[18] E. Nilsson, J. Berendson, E. Fontes, Development of a dosage method for electrochemical treatment of tumours: a simplified mathematical model, Bioelectrochem. Bioenerget. 47 (1998) 11–18, https://doi.org/10.1016/S0302-4598(98)00157-3.
[19] E. Nilsson, J. Berendson, E. Fontes, Impact of chlorine and acidification in the electrochemical treatment of tumours, J. Appl. Electrochem. 30 (2000) 1321–1333, https://doi.org/10.1023/A:1026560806158/METRICS.
[20] A.E.B. Pupo, M.M. González, L.E.B. Cabrales, J.B. Reyes, E.J.R. Oria, J.J.G. Nava, R.P. Jiménez, F.M. Sánchez, H.M.C. Ciria, J.M.B. Cabrales, 3d current density in tumors and surrounding healthy tissues generated by a system of straight electrode arrays, Math. Comput. Simul. 138 (2017) 49–64, https://doi.org/10.1016/J.MATCOM.2017.01.004.
[21] A. Soba, C. Suárez, M.M. González, L.E.B. Cabrales, A.E.B. Pupo, J.B. Reyes, J. P. Martínez Tassé, Integrated analysis of the potential, electric field, temperature, pH and tissue damage generated by different electrode arrays in a tumor under electrochemical treatment, Math. Comput. Simul. 146 (2018) 160–176, https://doi.org/10.1016/J.MATCOM.2017.11.006.
[22] A. Mokhtare, M. Shiv Krishna Reddy, V.A. Roodan, E.P. Furlani, A. Abbaspourrad, The role of pH fronts, chlorination and physicochemical reactions in tumor necrosis in the electrochemical treatment of tumors: a numerical study, Electrochim. Acta 307 (2019) 129–147, https://doi.org/10.1016/J.ELECTACTA.2019.03.148.
[23] D. Miklavčič, D. Šemrov, V. Valenčič, G. Serša, L. Vodovnik, Tumor treatment by direct electric current: computation of electric current and power density distribution, 10.3109/15368379709009837 16 (2009) 119–128. https://doi.org/10.3109/15368379709009837.
[24] J. Berendson, J.M. Olsson, Bioelectrochemical aspects of the treatment of tissue with direct current, 10.3109/15368379809012883 17 (2009) 1–16. https://doi.org/10.3109/15368379809012883.
[25] H. Von Euler, E. Nilsson, A.S. Lagerstedt, J.M. Olsson, Development of a dose-planning method for electrochemical treatment of tumors: a study of mammary tissue in healthy female CD rats, 10.3109/15368379909012903 18 (2009) 93–104. https://doi.org/10.3109/15368379909012903.
[26] R.L. Ren, N. Vora, F. Yang, J. Longmate, W. Wang, H. Sun, J.R. Li, L. Weiss, C. Staud, J.A. McDougall, C.K. Chou, Variations of dose and electrode spacing for rat breast cancer electrochemical treatment, Bioelectromagnetics 22 (2001) 205–211, https://doi.org/10.1002/BEM.40.
[27] E.M. Calzado, J.L.G. Rodríguez, L.E.B. Cabrales, F.M. García, A.R.S. Castañeda, I.M. G. Delgado, L.M. Torres, F.V.G. Uribazo, M.M. González, S.C.A. Brooks, T. R. González, E.J.R. Oria, L.L.B. Roger, H.E.H. Figueroa, G.D. Pérez, Simulations of the electrostatic field, temperature, and tissue damage generated by multiple electrodes for electrochemical treatment, Appl. Math. Model. 76 (2019) 699–716, https://doi.org/10.1016/J.APM.2019.05.002.
[28] M. Marino, N. Olaiz, E. Signori, F. Maglietti, C. Suárez, S. Michinski, G. Marshall, pH fronts and tissue natural buffer interaction in gene electrotransfer protocols, Electrochim. Acta 255 (2017) 463–471, https://doi.org/10.1016/J.ELECTACTA.2017.09.021.
[29] J.R. Garbay, V. Billard, C. Bernat, L.M. Mir, N. Morsli, C. Robert, Successful repetitive treatments by electrochemotherapy of multiple unresectable Kaposi sarcoma nodules, Eur. J. Cancer Suppl. 4 (2006) 29–31, https://doi.org/10.1016/J.EJCSUP.2006.07.005.